Multiple-scattering-free light scattering spectroscopy with mode selectivity

Shinsaku Takagi[1,2] and Hajime Tanaka[1,*]

[1]*Institute of Industrial Science, University of Tokyo, Meguro-ku, Tokyo 153-8505, Japan*

[2]*Faculty of Knowledge Engineering, Tokyo City University, Setagaya-ku, Tokyo 158-8557, Japan*

(Received 13 April 2009; revised manuscript received 7 January 2010; published 1 February 2010)

Seeing through the dynamics of turbid media is often demanded in both science and technology. Dynamic light scattering is one of the most powerful means to study the dynamics of various condensed matter systems, in particular, soft matter systems, in a nondestructive manner. However, its applicability is often limited by multiple scattering of light, which severely distorts the signal. To overcome this problem, cross correlation spectroscopy has been developed. Here, we propose another physical principle by which we can avoid the effects of multiple scattering. We demonstrate that this method allows not only Rayleigh but also Brillouin scattering measurements even in very turbid colloidal suspensions. This method opens a possibility of optically characterizing the dynamics (translational and rotational diffusion, thermal diffusion, and acoustic phonon dynamics) of turbid materials with mode selectivity.

I. INTRODUCTION

Light scattering has enjoyed a dominant role in characterizing various types of condensed matter, in particular, soft matter such as polymer solutions, colloidal suspensions, emulsions, liquid crystals, and solutions of biological molecules [1]. However, soft and bio matter are often turbid due to multiple scattering of light from congested internal structures, whose characteristic length is comparable to the wavelength of light. In other words, multiple scattering is inevitable for these systems, whose interesting characteristics arise from their mesoscopic length scale itself. However, light scattering is usually limited to optically transparent samples, and thus it is hard to apply this technique to spatially inhomogeneous materials, which strongly scatter light and thus are turbid. For a system of dilute scatterers, we may assume that incident light is scattered only once. For a system of dense scatterers, however, such an assumption is no longer valid and the detected light must be scattered twice or even more. Such multiple scattering becomes significant if the mean distance between two scattering events, i.e., the scattering mean free path, is substantially shorter than a sample size. In ordinary methods, both single- and multiple-scattered light enter into a photodetector and the resulting photocurrent is processed without discrimination. This mixing leads to the loss of information on the polarization direction and the scattering wave vector of the detected light, which causes fatal deformation of light scattering spectra [2]. In the limit of strong multiple scattering, on the other hand, the process of light scattering can be regarded as diffusive light propagation. In this limit, we can use so-called diffusive wave spectroscopy (DWS) [3–5]. However, this method, which directly uses multiply scattered light, does not provide dynamic structure factors in a direct way.

To isolate singly scattered light in a turbid sample, powerful methodologies have been developed [6–13]: mutual (or cross) correlation dynamic light scattering (DLS) [6] such as two-color DLS [8–10] and three-dimensional DLS (3DDLS) [11–13]. The basic principle of isolating singly scattered light is to perform two scattering experiments simultaneously on the same scattering volume and cross-correlate the signals obtained. If both experiments share the same scattering vector q but use different scattering geometries, only singly scattered light will produce correlated intensity fluctuations on both detectors. In contrast, multiply scattered light, scattered in a succession of generally different q vectors, results in uncorrelated fluctuations, which contribute to the background only. This method is very powerful for measuring translational diffusion modes, but their applications to other dynamic modes such as rotational and thermal diffusion and acoustic phonons are very difficult and rare. Furthermore, sharing exactly the same scattering vector q and the same scattering volume in the simultaneous two scattering measurements is technically demanding.

In this paper, we propose another type of multiple scattering free DLS, which is based on a physical principle essentially different from that of the cross correlation DLS. Unlike the cross correlation DLS, which requires simultaneous two scattering experiments as described above, we need only one scattering experiment. Our method is based on a DLS method, which we recently developed originally: phase-coherent light scattering (COLS) spectroscopy [14–18]. Here, we extend this method to translational diffusion measurements. More importantly, we demonstrate that a coherent phase-sensitive detection of scattered light allows us to reject multiply scattered light and pick up only light scattered once; that is, COLS is "intrinsically" free from multiple scattering effects. We emphasize that COLS can be applied to various dynamic modes including translational, rotational, and thermal diffusion and acoustic phonons. Examples of multiple scattering free phase-coherent Rayleigh (CORS) and Brillouin scattering (COBS) are demonstrated below.

The organization of this paper is as follows. In Sec. II, we describe the physical principle of COLS for translational diffusion measurements. In Sec. III, we explain the optical setup and the details of experiments. In Sec. IV, we report our experimental results and discuss them. In Sec. V, we
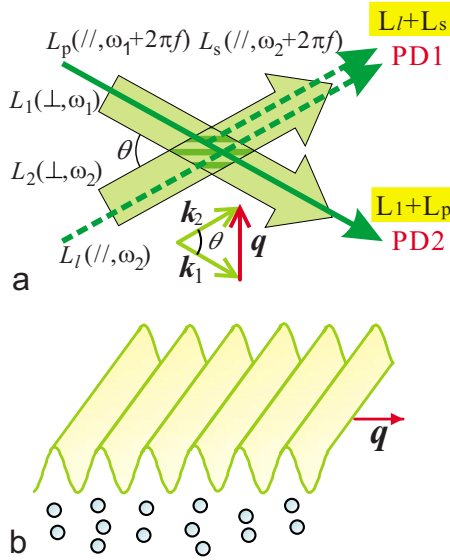
---

*tanaka@iis.u-tokyo.ac.jp

FIG. 1. (Color online) (a) Principle of producing a dynamic light-field grating. $\mathbf{k}_1$ and $\mathbf{k}_2$ are the wave vectors of pump beams L_1 and L_2, respectively. L_p is the probe beam. L_p is scattered by the material grating produced by the light-field grating induced by the pump beams L_1 and L_2 [see (b)]. L_s is the scattered light with the wave vector $\mathbf{k}_2$. L_l is the local light, which is mixed with L_s on a photodiode PD1. We also mix L_1 with L_p, whose polarization direction is slightly rotated by a polarizer, on a photodiode PD2, to produce a reference signal for a phase-sensitive two-phase lock-in detection. See text on the details. (b) Schematic figure of the excitation of coherent concentration modulation. Propagating modulated light field and the resulting modulation of a colloid concentration are shown.

compare our method with mutual correlation spectroscopy. In Sec. VI, we summarize our study.

II. PHYSICAL PRINCIPLE OF COLS FOR TRANSLATIONAL DIFFUSION MEASUREMENTS

A. COLS for translational diffusion measurements

First, we explain the principle of our method to measure translational diffusion of particles, using colloidal suspensions as an example. We generate a moving interference pattern in a colloidal suspension by crossing two continuous wave (cw) laser beams [L_1 and L_2, see Fig. 1(a)], whose frequencies differ slightly by ω. These pump beams L_1 and L_2 produce a moving interference pattern. The polarization directions of these pump beams are both vertical ($\perp$). Since the frequency difference ω is much smaller than the light frequencies (~ 500 THz), the wave numbers of the two beams have almost the same value of the wave number k. Thus, the wave vector difference can be expressed as $q = |\mathbf{q}| = 2k \sin(\theta/2)$, where θ is the beam-crossing angle. Due to the interference of the two beams, the light intensity of the beam-crossing region is modulated as $\delta I(\mathbf{r}, t) = \mathrm{Re}[2E_1 E_2 e^{i(\mathbf{q} \cdot \mathbf{r} - \omega t)}]$, where $E_i (i = 1, 2)$ is the electric field strength of the pump beam L_i. Consequently, a moving interference pattern with a phase velocity of ω/q is produced in the sample.

In the beam-crossing volume, the laser-field potential affects the motion of colloidal particles. The optically modulated chemical potential is given by [19]

$$\mu = \mu_0 - \frac{1}{2}\left(\frac{\partial \epsilon}{\partial \rho}\right)_T \delta I, \qquad (1)$$

where μ_0 and ϵ are the chemical potential and the dielectric constant of a suspension in the absence of the optical field, and ρ is the density of the suspension. Note that for a low particle concentration, $\left(\frac{\partial \epsilon}{\partial \rho}\right)_T = \frac{3(m^2-1)}{m^2+2}\frac{\epsilon_1}{\Delta\rho}$, where m is the ratio of the refractive index of particles to that of the solvent, ϵ_1 is the dielectric coefficient of the solvent, and $\Delta\rho$ is the density difference between the particles and the solvent. The optical potential tends to force particles to migrate into a region of stronger (weaker) light intensity if the refractive index of the particles is higher (lower) than the solvent. Thus, particles tend to form a periodic concentration pattern, following the moving interference pattern [see Fig. 1(b)]. In other words, particles are driven by the periodically modulated moving interference pattern. However, if the pattern moves too quickly, the particle concentration diffusion mode cannot follow it. This situation can be described by the following dynamic equation of the colloidal concentration c, which is derived by substituting Eq. (1) to the diffusion equation $\partial c/\partial t = M\nabla^2\mu$, where M is the transport coefficient of a particle

$$\partial c/\partial t = D_c \nabla^2 c - (1/2)(\partial\epsilon/\partial\rho)\nabla^2 \delta I,$$

where $D_c = M(\partial\mu_0/\partial c)_T$ is the translational collective diffusion coefficient of colloids. Here, we note that we consider only a linear response regime in the above. Then, the complex spectra of a particle diffusion mode, which is proportional to the Fourier transformation of the concentration modulation, is given by

$$\delta c(\mathbf{q}, \omega) = \frac{\left(\frac{\partial \epsilon}{\partial \rho}\right)_T q^2}{-i\omega + D_c q^2} E_1 E_2. \qquad (2)$$

From the spectra, we can obtain D_c, which satisfies the Stokes-Einstein relation for a dilute sample: $D_c \cong D_0 = k_B T/(6\pi\eta a)$, where D_0 is the self-diffusion constant for a single particle, k_B is Boltzmann's constant, η is the viscosity of a solvent, and a is the particle radius. In the above, we ignore complex many-body interactions such as long-range Coulomb and hydrodynamic interactions, which allows us to use the above simplified diffusion equation and assume $D_c \cong D_0$. These interactions are known to produce profound features in D_c [20]. Here, we emphasize that our measurement principle relies solely on the fluctuation-dissipation (i.e., linear response) theorem [14] and thus our method should provide the correct complex spectra $\delta c(\mathbf{q}, \omega)$ for any situations with complex many-body interactions, although the simple Lorentzian form, Eq. (2), may no longer be valid.

B. Superheterodyne phase-sensitive detection of light

Next, we describe how to detect the above concentration diffusion mode as complex spectra. We introduce the probe

beam L_p with the horizontal polarization direction //, collinearly to the pump beam L_1. This probe beam L_p(//) with the wave vector $\mathbf{k}_1$ is scattered by the above-mentioned collective mode of translational diffusion of colloids, δc. Since the Bragg diffraction condition between the probe beam and the excited concentration grating is automatically satisfied, the path of the scattered beam L_s(//) is exactly on that of L_2. Then, the scattered light L_s(//) with the wave vector $\mathbf{k}_2$ is mixed on a photodiode PD1 with a local light L_l(//) with the wave vector $\mathbf{k}_2$, which is set collinearly to the pump beam L_2 and has the horizontal polarization direction. By detecting the beat signal produced by mixing L_s and L_l on the photodiode PD1, including its phase, we can obtain the complex spectra given by Eq. (2) (see below).

Now, we explain the details of our optical superheterodyne phase-sensitive detection method [14,17,21,22]. The angular frequencies of the excitation beams L_1 and L_2 are, respectively, ω_1 and ω_2. The probe beam L_p is from the same light source with the angular frequency shifted by f, that is, $\omega_p = \omega_1 + 2\pi f$, while the local light L_l is from the same light source with the same angular frequency ω_2. We also define E_p and E_l, respectively, as the electric field strength of the probe (L_p) and local light (L_l). The probe light L_p is scattered by coherent modes produced by crossing the two laser beams L_1 and L_2. The angular frequency of the excited modes is $\omega = \omega_2 - \omega_1$. A component of the scattered electrical field at the detector position $\mathbf{R}$, $E_s(\mathbf{R},t)$, is given by [1]

$$E_s(\mathbf{R},t) = \frac{-k_s^2 E_p V}{4\pi\epsilon_0 R}\left(\frac{\partial\boldsymbol{\epsilon}}{\partial c}\right)_T (\boldsymbol{n}_p \cdot \boldsymbol{n}_s) \times e^{i(k_s \cdot \mathbf{R} - \omega_s t)}\delta c(\boldsymbol{q},\omega).$$
(3)

Here, $\boldsymbol{n}_i$ is the unit vector of the polarization direction of light beam i. The angular frequency of the scattered light L_s, ω_s, satisfies $\omega_s = \omega_p + \omega = (\omega_1 + 2\pi f) + (\omega_2 - \omega_1) = \omega_2 + 2\pi f$. Since the total electric field on the photodiode PD1 is given by the summation of the local light L_l (polarization $\boldsymbol{n}_l$) and scattered one L_s [polarization $\boldsymbol{n}_s(=\boldsymbol{n}_l)$] as $\boldsymbol{E}(\mathbf{R},t) = \boldsymbol{n}_s[E_l e^{-i\omega_2 t} + E_s(\mathbf{R},t)]$, we obtain the output current of the photodiode PD1, i_{out}, as

$$i_{out}(t) = g\boldsymbol{E}\cdot\boldsymbol{E}^* = dc + 2g\left[\frac{k_s^2}{8\pi\epsilon_0 R}\frac{\partial\boldsymbol{\epsilon}}{\partial c}(\boldsymbol{n}_p\cdot\boldsymbol{n}_s)E_l E_p\right.$$
$$\times \{\text{Re}[\delta c(\boldsymbol{q},\omega)]\cos(2\pi f t)$$
$$\left.- \text{Im}[\delta c(\boldsymbol{q},\omega)]\sin(2\pi f t)\}\right],$$
(4)

where g is the quantum efficiency of the optical detector (PD1), k_s is the wave number of the scattered light, $R = |\mathbf{R}|$, and ϵ_0 is the dielectric constant of vacuum. Thus, the two-phase lock-in detection of i_{out} with a reference signal of $\cos(2\pi f t)$ gives us $\text{Re}[\delta c(\boldsymbol{q},\omega)]$ and $\text{Im}[\delta c(\boldsymbol{q},\omega)]$, respectively, as the in-phase and out-of-phase components of the signal. We use the beat signal produced by mixing L_1 and L_p on the photodiode PD2 as the reference signal, which is proportional to $\cos(2\pi f t)$. To produce such a beat signal with L_1, we slightly change the polarization direction of L_p by a polarizer, before mixing. This is because the polarization direction of L_p is perpendicular to that of L_1 and thus they do not produce a detectable beat signal on PD2 if we mix them as they are.

This phase-sensitive detection of the coherent scattering signal provides us with an ultimate signal-to-noise ratio and also with complex spectra of an excited dynamic mode [16]. It should be noted that we can eliminate all of the incoherent components of scattered light by this detection method. This feature is crucial for multiple scattering free measurements. In conventional phase-insensitive heterodyne methods [21–24] on the other hand, only the power spectrum $|\delta c(\boldsymbol{q},\omega)|^2$ can be obtained. There, the square-law detected signal through the bandpass filter is measured as a function of frequency; a spectrum analyzer has often been used for this purpose. In this method, the light scattered by incoherent fluctuations cannot be eliminated.

Finally, we note that around the beam-crossing angle of $\pi/2$, there is only a very weak signal because $\boldsymbol{n}_p \cdot \boldsymbol{n}_s$ becomes very small in Eq. (4) for $\theta \sim \pi/2$.

C. Physical principle for multiple scattering free light scattering

Next, we explain the key principle that makes our method free from multiple scattering effects. In our method, a coherent concentration modulation is created by the moving interference pattern. Its modulation frequency $\omega = \omega_2 - \omega_1$ is determined by the frequency difference of the two laser beams crossed in a sample. So, the frequency shift upon single scattering by a coherent modulation mode amounts to ω. The frequency shift upon multiple scattering is usually very different from that of single scattering. Thus, we can easily distinguish them in terms of the amount of the frequency shift in scattered light. We can pick up only a signal with the modulation frequency ω using lock-in detection. Even if there exist multiply scattered light components of the completely same frequency and wave vector as those of the coherent mode, the phases of the multiply scattered components are randomized and incoherent with respect to the excited coherent mode. Thus, the phase-sensitive detection of the scattered light can completely reject the multiply scattered components.

III. EXPERIMENTAL

A. Phase-coherent light scattering method

The basic principle of phase-coherent light scattering spectroscopy was described in Refs. [14,15]. Here, we describe the optical setup and the signal processing for CORS and COBS.

1. CORS method

We show the optical configuration for measuring the translational diffusion by CORS in Fig. 1(a) and a block diagram in Fig. 2 (see also [17,18]). For CORS measurements, we used a continuous wave, frequency doubled Nd:YAG laser (532 nm) (Verdi-V2, Coherent Inc.). We used the maximum power of this laser, 2 W, which provides the best signal-to-noise ratio. We confirmed that this laser power
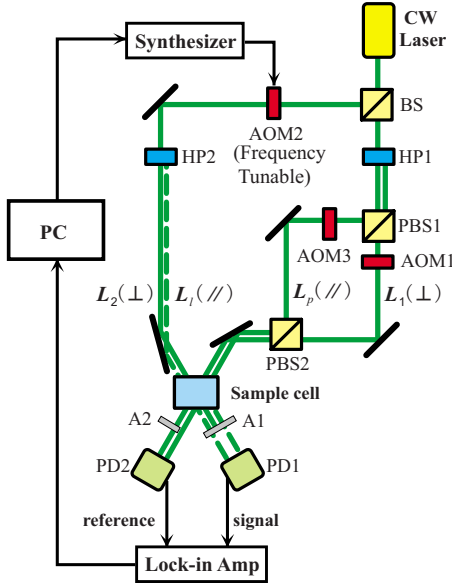
FIG. 2. (Color online) A block diagram of our COLS system. BS stands for beam splitter, PBS1 and PBS2 for polarizing beam splitters, AOM1–3 for acousto-optic modulators, PD1 and PD2 for photodetectors, A1 and A2 for analyzers (polarizing plates), HP1 and HP2 for $\lambda/2$ plates, and PC for a computer. ∥ indicates light with horizontal polarization, while ⊥ does light with vertical polarization.

causes neither damage to our samples nor local heating due to light absorption. A vertically polarized beam radiated from the laser source is first divided into three beams, two of which work as the pump beams, L_1 and L_2, and generate the laser-field grating in the beam-crossing region [see Fig. 1(a)]. L_1 and L_2 have vertical polarization. We used a frequency-tunable acousto-optic modulator (AOM2) to shift the optical frequency of L_2 by ω from the original one. Thus, we can change the beat frequency of the laser-induced grating by scanning ω. Using the half-lambda plate (HP1) and the polarizing beam splitters (PBS1 and 2), we also made the third beam, whose polarization direction is rotated by 90°. This beam works as the probe beam L_p with horizontal polarization, entering a sample and then scattered by the excited coherent grating. The probe beam L_p is set collinearly to the pump beam L_1 before entering the liquid sample. Thus, the Bragg diffraction condition between the probe beam and the excited concentration grating is automatically satisfied so that the path of the scattered beam is exactly on that of L_2.

In order to scan the frequency of the laser-induced grating, $\omega/2\pi$, we must control the frequency of L_2, $\omega_2/2\pi$, within the frequency range of ± 1 MHz around that of L_1, $\omega_1/2\pi$. We accomplish this by using acousto-optic modulators, one of which (AOM2) is frequency tunable. These pump beams pass through the acousto-optic modulator to cause the fixed frequency shift of 80 MHz for L_1 and the variable frequency shift of around 80 MHz for L_2, respectively. The frequency of the acousto-optic modulator (AOM2) for L_2 is tuned by scanning its driver frequency. We control the driver frequency by using an external oscillation signal of an rf synthesizer (HP8648A, Hewlett-Packard) as the input. It should be noted that a diffraction angle of the

laser beam through the acousto-optic modulator changes if the modulation frequency is varied. The actual change in the diffraction angle is, however, much less than 1 mrad when the frequency range scanned is within ± 1 MHz. Therefore, this change in the diffraction angle does not affect the heterodyne beat efficiency and thus it is negligible for our Rayleigh scattering measurements. The frequency resolution of our CORS system is less than 100 Hz, which is determined by the frequency stability of the synthesizer and the acousto-optic driver and, more seriously, by mechanical oscillations of the measurement system.

We also put the third acousto-optic modulator (AOM3) on the path of probe beam L_p to cause the frequency shift of 82 MHz. The resulting small frequency difference ($f=2$ MHz) between L_1 and L_p is necessary for measuring the real and imaginary parts of $\delta c(\mathbf{q}, \omega)$ separately, instead of the power spectrum $|\delta c(\mathbf{q}, \omega)|^2$. The frequency difference f acts as the reference frequency of our optical superheterodyne detection method. As explained in Sec. II B, first, we slightly change the polarization direction of L_p by a polarizer (A2) to make its ⊥ component, which is necessary to create a beat signal between L_1 and L_p. By mixing $L_1(\perp)$ and $L_p(/\!/)$ on the photodiode PD2, the reference signal with frequency f is produced and fed into the reference input for the lock-in amplifier.

The scattered light L_s is mixed with the local light L_l with horizontal polarization to produce the beat signal of a fixed frequency ($f=2$ MHz) by a Si PIN photodetector PD1 (S6468, HAMAMATSU Photonics). The intensity of L_l is set to be weak enough to avoid the saturation of the photodiode PD1. The lock-in detection of the photocurrent of PD1 with respect to the reference signal of $\cos(2\pi ft)$ (see above) gives us real and imaginary parts, respectively, as the in-phase and out-of-phase components of the signal (see B below). For the detection of the signal by the reference frequency of 2 MHz we used a two-phase lock-in amplifier (model 200, Palo Alto Research), and a lock-in extender (model PAR 100, Palo Alto Research).

2. COBS method

Figure 3 shows the optical setup of COBS, which is the same as CORS except the lasers [16]. For Brillouin scattering measurements, we need a moving interference pattern which propagates with the speed of a phonon frequency. Typically the frequency of acoustic phonons ranges from MHz to GHz. This means that the frequency difference between L_1 and L_2 should be changed in this range. So we use two frequency-tunable single-mode cw green (532 nm) lasers (Diabolo, Innolight GmbH), which have a frequency tunability over 10 GHz without mode hopping, the extremely high frequency stability (spectral linewidth <1 kHz/min; frequency stability <2 MHz/min), and the high power (1 W). The frequency difference of the two lasers is electrically controlled by a computer. The other setup is basically the same as CORS. See Ref. [16] for the details of the system.

B. Photon Correlation Spectroscopy

In order to verify the elimination of multiple scattering in our method we also performed conventional DLS measure-
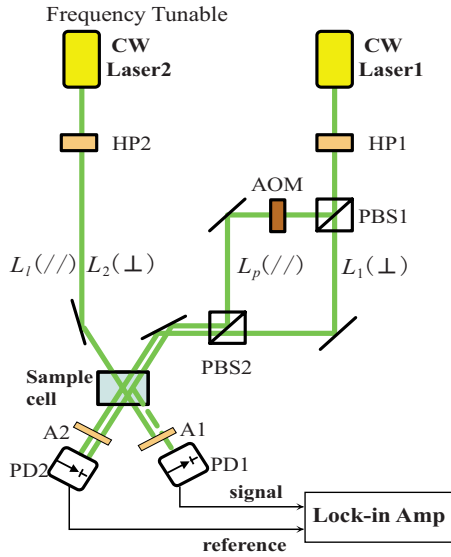
FIG. 3. (Color online) A block diagram for COBS. The meaning of the symbols is the same as in Fig. 2. The only difference is that we use frequency-tunable lasers for this experiment.

ments to obtain a normal autocorrelation function in a time domain using the other light source with the same wavelength of 532 nm (Compass 315M, Coherent Inc.), photomultiplier and a photon correlator (ALV-5000, ALV GmbH).

C. Samples

Colloids used were monodisperse poly(styrene) (PS) latex particles (purchased from PolyScience, Inc.). They are suspended in pure water. We prepared suspensions of particles of 48, 64, 107, 174, 200, and 300 nm diameter with various concentrations between 0.001 and 2.5 wt%. They were stable without aggregation for more than two months, although some degree of sedimentation slowly takes place.

We note that the refractive index of polystyrene latex is 1.58 and that of water is 1.34 at 532 nm. This rather large mismatch of the refractive index allows us to study the effects of multiple scattering at rather low colloid concentrations ($c_0 \leq 1$ wt%). Because of this feature, we can investigate multiple scattering effects in a concentration range, where we can neglect complex many-body interactions such as long-range Coulomb interactions and hydrodynamic interactions. This simplifies the analysis of our light scattering spectra (see below).

D. Sample cell

Since the turbidity of a sample depends on the particle size, the concentration, and the cell thickness, we chose a sample cell with a proper thickness for each sample to observe the spectra while keeping sufficient light intensity. We used a rectangular glass cell with the optical path length of 1 mm for weakly turbid samples, whereas a glass cell with the path length of 0.5 mm for strongly turbid samples. All the experiments were performed at room temperature.

E. Experimental details

We changed the scattering angle by crossing two beams ($L_1 + L_p$ beam and $L_2 + L_l$ beam) with an angle ranged from 10° to 170°. First, we cross the two beams without a cell. Then, we set a cell so that a glass surface of the cell becomes perpendicular to the $L_1 + L_p$ beam. To minimize the inaccessible q range due to the rectangular shape of a cell (see also below), we also use an oblique incidence. The real scattering angle is changed due to the refraction of another light beam, which is estimated from the refractive indices of the cell wall and the sample. See also Ref. [25] for a way to change the scattering angle in a systematic way.

For COLS, we cannot measure the scattering signals for a scattering angle θ around 90°. This is why we do not have any data in Fig. 5(b) for the q^2 range of $4.4 \sim 7.0 \times 10^{10}$ m^{-2}. As described above, this is because in COLS the scattering intensity is proportional to $\boldsymbol{n}_p \cdot \boldsymbol{n}_s$ [see Eq. (4)], which becomes very small for $\theta \sim \pi/2$. This is an intrinsic deficiency of COLS coming from its physical principle.

IV. RESULTS AND DISCUSSION

A. Multiple-scattering-free COLS

We now show results of measurements of a particle (concentration) diffusion mode by this method. The block diagram of our CORS system is shown in Fig. 2. Typical complex spectra of a colloidal suspension are shown in Fig. 4(a). The real and imaginary parts correspond to those of Eq. (2), respectively. This is the first observation of complex DLS spectra of a concentration diffusion mode. In this measurement, the sample was a 0.1 wt% aqueous suspension of latex particles of $a = 54$ nm and the sample cell was 1 mm. We emphasize that for this condition, there are significant multiple scattering effects. Note that even for a more dilute sample (the colloidal concentration $c_0 = 0.05$ wt%) the dispersion relation measured by ordinary photon correlation spectroscopy is already strongly distorted [see Fig. 5(a)]. The least square fitting of a Lorentzian function [see Eq. (2)] to both real and imaginary parts of the spectra yields $D_{\text{coll}} = 5.01 \times 10^{-8}$ cm^2/s [see Fig. 4(b)]. On the other hand, from the relation $D_{\text{coll}} = k_B T/(6\pi\eta a)$ with $T = 288$ K and $\eta = 7.97 \times 10^{-4}$ Pa·s, we estimate $D_{\text{coll}} = 4.94 \times 10^{-8}$ cm^2/s, which agrees very well with the above measured value. Furthermore, the slope of the line in Fig. 4(b), which shows the particle-size dependence of D_{coll}, yields $k_B T/6\pi\eta = 2.60 \times 10^{-13}$ cm^3/s, which is also consistent with the theoretical value (2.65×10^{-13} cm^3/s).

Next, we compare the characteristic decay time τ obtained from the half width at half maximum (HWHM) of complex spectra with that from photon correlation spectroscopy. In the latter, which is a time-domain measurement, we can obtain an autocorrelation function of scattered light intensity, which is expressed as $g_2(t) = 1 + \exp(-2t/\tau)$. Provided that many-body interactions are neglected, τ^{-1} should be proportional to q^2 for a diffusion mode. Figure 5(a) shows the q^2 dependence of τ^{-1} obtained from the photon correlation function of colloidal suspensions ($a = 54$ nm) for three con-
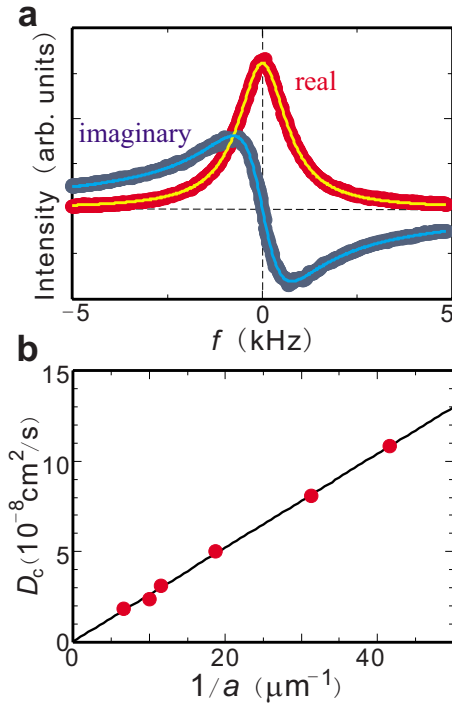
FIG. 4. (Color online) Measurements of translational collective diffusion. (a) Typical complex spectra of a PS latex aqueous suspension (a=54 nm, c_0=0.1 wt%, and the cell thickness=1 mm) in a back scattering configuration (θ=175°). HWHM was 770 Hz. The frequency resolution bandwidth was set to be 200 Hz. The solid lines are the fitted theoretical curves [see Eq. (2)]. (b) Stokes-Einstein relation of PS suspensions of various particle sizes (c_0=0.1 wt% for all). Straight line shows the result of the least square fitting of the relation: $D_c=(k_B T/6\pi\eta)(1/a)$.

centrations (c_0=0.05, 0.2, and 1.0 wt%). For the low concentration range studied here, we expect a linear relationship between τ^{-1} and q^2, but the relation is already distorted even for c_0=0.05 wt%. As the concentration increases, τ^{-1} more and more severely deviate from the linear relationship. For a sample of c_0=1.0 wt%, the shape of the correlation function itself deviates from the single exponential decay and thus even the value of τ cannot be determined accurately [see red triangles in Fig. 5(a)]. This nonideal behavior is due to multiple scattering effects [2]. Multiple scattering leads to a broad distribution of the diffusion time τ even for a monodisperse sample, due to the mixing of information of various wave vectors and polarizations. We note that a sample of c_0=1.0 wt% in a 0.5-mm-thick cell looks milky and only less than 10% of the incident light is transmitted [see Fig. 5(c)]. The ordinary light scattering method cannot distinguish singly scattered light from multiply scattered light and thus are inevitably subject to multiple scattering effects for such turbid samples.

Contrary to this, our COLS method allows us to accurately measure physically meaningful spectra even for turbid samples, as mutual correlation spectroscopy does. This is because we can selectively detect only singly scattered light, which preserves the information on the polarization and the wavenumber of light, and reject multiply scattered light. Figure 5(b) shows results of a COLS measurement of a sample
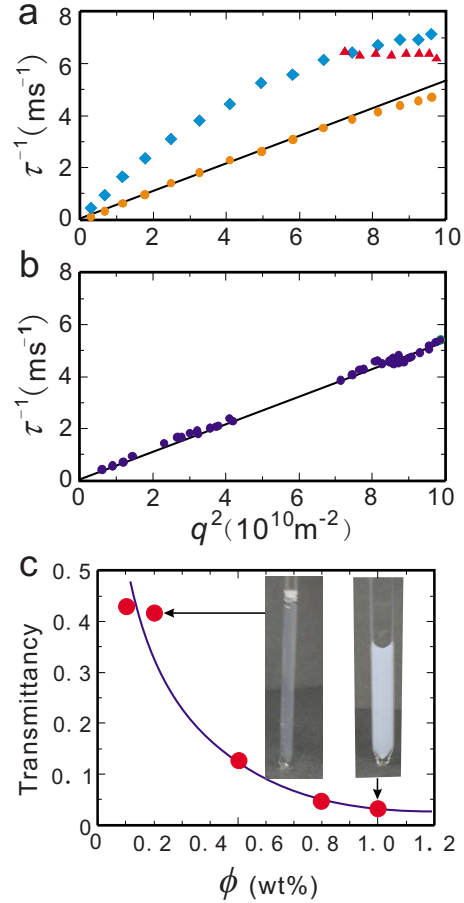

FIG. 5. (Color online) Dispersion relations of PS latex aqueous suspensions. The samples are suspensions of PS latex (a=54 nm). (a) Dispersion relations measured by conventional (photon counting) dynamic light scattering spectroscopy, which deviates from the expected relation (solid line). The concentrations of suspensions are 0.05 (orange circles), 0.2 (blue diamonds), and 1.0 wt% (red triangles), respectively. (b) Dispersion relation measured by CORS for the 1.0 wt% suspension (a=54 nm). The expected relation $\tau^{-1}\propto q^2$ (solid line) holds quite well even under strong multiple scattering. (c) Transmittance of the incident light in PS aqueous suspensions (a=54 nm). The photographs of samples in optical cells, which are used for light scattering measurements, are also shown for the two concentrations (0.2 and 1 wt%).

of c_0=1.0 wt%, through which only less than 10% of the incident light can pass [see Fig. 5(c)]. Unlike the above-described results of the ordinary photon correlation spectroscopy, τ^{-1} is almost perfectly proportional to q^2, indicating that our measurement is indeed free from multiple scattering effects.

B. Multiple-scattering-free COBS

The above principle of multiple scattering free measurements should also apply to other dynamic modes, which can be measured by COLS [14,15]. These modes include thermal diffusion (polarized Rayleigh scattering) [14,18], rotational diffusion (depolarized Rayleigh scattering) [15,18], and sound propagation (Brillouin scattering) [14,16,18]. Here,
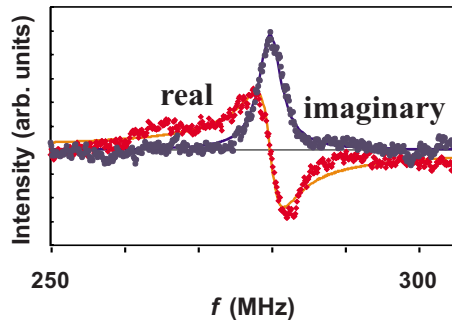
FIG. 6. (Color online) Complex Brillouin spectra measured for a turbid colloidal suspension (c_0=0.5 wt% and a=54 nm) at T=20 °C. The sample was filled in a cell of 1 mm thickness, and the optical transmission was 12.6%. The scattering angle was 5.75° (q=1886 cm^{-1}). The phonon frequency and the HWHM were determined to be 280 and 3.5 MHz, respectively, by fitting the theoretical curves (solid lines). The frequency resolution bandwidth was set to be 2 MHz.

we show an example of multiple scattering free phase-coherent Brillouin scattering (COBS) measurements. As shown in Fig. 6, the complex Brillouin spectra are successfully observed with an extremely high frequency resolution even in a very turbid colloidal suspension, through which only about 10% of the incident light can pass. The sound velocity is estimated as 1485 m/s, which is almost the same as that of water as expected for a long wavelength limit of a dilute suspension. This clearly indicates that COLS can indeed be free from multiple scattering for any dynamic modes. We emphasize that the frequency resolution of COBS is much higher (nearly a factor of 100) than conventional methods using a Fabry-Pérot interferometer.

V. COMPARISON BETWEEN COLS AND CONVENTIONAL MUTUAL CORRELATION SPECTROSCOPY

Here, it may be worth comparing COLS and mutual correlation spectroscopy (MCS) [3,6–13]. Although both COLS and MCS can remove multiple scattering contributions, the principle is very different between them. In COLS, multiple scattered light causes a beat frequency different from ω and, more importantly, loses phase coherence with respect to the optically excited coherent mode and thus it can be completely removed by the phase-sensitive (lock-in) detection of the scattered light at the frequency ω, as described above. In MCS, on the other hand, multiple scattering contributions to temporal correlation functions are decorrelated by performing two geometrically different scattering experiments simultaneously on the same scattering volume at identical $\boldsymbol{q}$. This relies on that multiply scattered light is generally determined at wave vectors different from $\boldsymbol{q}$ and thus uncorrelated. This basic principle is the same between two-color [8–10] and three-dimensional DLS [11–13]. This principle requires a rather complicated optical setup. More precisely, the intercept of the cross correlation function decreases with an increase in the mismatch of $\boldsymbol{q}$ and/or the scattering volumes.

Thus, a very precise alignment is required, particularly for two-color DLS. Our method is rather free from such a complicated alignment for scattering, which comes from the requirement for performing two scattering experiments simultaneously in MCS. Although our optical setup is also complex due to the usage of four light beams, it is rather easy to change the scattering angle once we prepare the two collinearly aligned beams, the L_1+L_p and L_2+L_l beam.

It may be worth noting that there is a difference in the frequency range covered between COLS and MCS. Our COLS method uses a (super)heterodyne detection, which typically covers from about 100 Hz to 10 GHz. On the other hand, mutual correlation spectroscopy usually uses a digital photon counting method and calculates the cross correlation between signals from two detectors: It typically covers from 10^4 s to 10^{-6} s. Thus, MCS and COLS are more suitable for slow and fast dynamic phenomena, respectively. So, it is fair to say that the two methods are complementary. We note that this feature of COLS allows us to apply it for Brillouin scattering (fast dynamics).

Finally, we emphasize that our method has mode selectivity (see [17,18]), but this feature is absent in MCS. The physical principle of our method clearly tells us that signals which are not coherent with respect to the excited coherent mode are completely rejected by phase-sensitive lock-in detection of the scattered light. We previously show the mode selectivity of our method in [17,18]. In these particular examples, we have succeeded in selectively measuring a thermal diffusion mode in the isotropic phase of a liquid crystal near its nematic transition, where strong incoherent critical orientational fluctuations overwhelm a thermal diffusion mode. In such a situation, a thermal diffusion mode cannot be measured by conventional light scattering spectroscopy. In our method, however, we can pick up only a coherent thermal diffusion mode excited by the crossed laser lights and reject incoherent lights from orientational fluctuations by phase-sensitive lock-in detection.

VI. SUMMARY

In summary, we developed a "multiple scattering free" phase-coherent light scattering method. Its validity is shown for both translational collective diffusion and longitudinal acoustic phonon measurements. Since this method picks up only the signal coherent to the optical excitation, it can reject signals from incoherent random fluctuations of thermal origin in a sample and thus has mode selectivity [17,18] as well as the multiple scattering free feature. This allows us to select only one of translational, rotational and thermal diffusion and acoustic phonon modes and measure its complex spectra even in a turbid sample. Concerning measurements of translational collective diffusion, our method may be comparable to the conventional mutual correlation spectroscopy. However, there is a difference in the frequency range covered: mutual correlation spectroscopy and COLS is more suitable for slow and fast dynamic phenomena, respectively. The mode selectivity and the applicability of COLS to various modes including acoustic phonons may be advantages over conventional mutual correlation spectroscopy.

Our method enables us to investigate various dynamic modes with *mode selectivity* in turbid systems, i.e., spatially heterogeneous materials such as concentrated suspensions of colloids, emulsions, liquid crystals, foams, dense solutions of biological molecules, and turbid solid composite materials. Such materials are important not only in basic science but also in industrial and biological applications. We note that although the examples presented here are soft matter, our method may also be applied to hard matter (e.g., dynamics of thermal diffusion and acoustic phonons).

[1] B. J. Berne and R. Pecora, *Dynamic Light Scattering* (Wiley, New York, 1976).

[2] C. M. Sorensen, R. C. Mockler, and W. J. O'Sullivan, Phys. Rev. A **14**, 1520 (1976); **17**, 2030 (1978).

[3] G. Maret and P. E. Wolf, Z. Phys. B: Condens. Matter **65**, 409 (1987).

[4] D. J. Pine, D. A. Weitz, P. M. Chaikin, and E. Herbolzheimer, Phys. Rev. Lett. **60**, 1134 (1988).

[5] D. J. Durian, D. A. Weitz, and D. J. Pine, Science **252**, 686 (1991).

[6] G. D. J. Phillies, J. Chem. Phys. **74**, 260 (1981); Phys. Rev. A **24**, 1939 (1981).

[7] J. K. G. Dhont, C. G. De Kruif, and A. Vrij, J. Colloid Interface Sci. **105**, 539 (1985).

[8] M. Drewel, J. Ahrens, and U. Podschus, J. Opt. Soc. Am. A **7**, 206 (1990).

[9] K. Schatzel, J. Mod. Opt. **38**, 1849 (1991).

[10] P. N. Segré, W. van Megen, P. N. Pusey, K. Schätzel, and W. Peters, J. Mod. Opt. **42**, 1929 (1995).

[11] C. Urban and P. Schurtenberger, J. Colloid Interface Sci. **207**, 150 (1998).

[12] C. Urban, S. Romer, F. Scheffold, and P. Schurtenberger, Macromol. Symp. **162**, 235 (2000).

[13] C. Sinn, R. Niehüser, E. Overbeck, and T. Palberg, Part. Part. Syst. Charact. **16**, 95 (1999).

[14] H. Tanaka and S. Takagi, J. Chem. Phys. **114**, 6286 (2001).

[15] S. Takagi and H. Tanaka, J. Chem. Phys. **114**, 6296 (2001).

[16] H. Tanaka, T. Sonehara, and S. Takagi, Phys. Rev. Lett. **79**, 881 (1997).

[17] S. Takagi and H. Tanaka, Rev. Sci. Instrum. **73**, 3337 (2002).

[18] S. Takagi and H. Tanaka, Phys. Rev. Lett. **93**, 257802 (2004).

[19] L. D. Landau and E. M. Lifshitz, *Electrodynamics of Continuous Media*, 2nd ed. (Addison-Wesley, Reading, MA, 1984).

[20] A. J. Banchio and G. Nägele, J. Chem. Phys. **128**, 104903 (2008); R. Simon, T. Palberg, and P. Leiderer, *ibid.* **99**, 3030 (1993); D. Reinke, H. Stark, H.-H. von Grunberg, A. B. Schofield, G. Maret, and U. Gasser, Phys. Rev. Lett. **98**, 038301 (2007).

[21] H. Tanaka and T. Sonehara, Phys. Rev. Lett. **74**, 1609 (1995).

[22] H. Tanaka and T. Sonehara, Rev. Sci. Instrum. **73**, 1998 (2002).

[23] H. Z. Cummins and H. L. Swinney, in *Progress in Optics*, edited by E. Wolf (North Holland, Amsterdam, 1970), Vol. 8, p. 133.

[24] D. Eden and H. L. Swinney, Opt. Commun. **10**, 191 (1974).

[25] T. Sonehara and H. Tanaka, Rev. Sci. Instrum. **73**, 263 (2002).